buildings

MDPI

Article

Effect of Silica Fume Concentration and Water–Cement Ratio on the Compressive Strength of Cement-Based Mortars

Maria M. Badalyan [1], Nelli G. Muradyan [1], Roza S. Shainova [1], Avetik A. Arzumanyan [1], Marine A. Kalantaryan [1], Rafayel R. Sukiasyan [1], Mkrtich Yeranosyan [2], David Laroze [3], Yeghiazar V. Vardanyan [1] and Manuk G. Barseghyan [1,*]

[1] Faculty of Construction, National University of Architecture and Construction of Armenia, 105 Teryan Street, Yerevan 0009, Armenia; marya.badalyan@mail.ru (M.M.B.); nellimuradyan06@gmail.com (N.G.M.); rozetta_11@mail.ru (R.S.S.); avetikarzumanyan@gmail.com (A.A.A.); kalantaryanm@mail.ru (M.A.K.); rafo.sukiasyan@gmail.com (R.R.S.); e_vardanyan2002@yahoo.fr (Y.V.V.)

[2] Innovation Center for Nanoscience and Technologies, A.B. Nalbandyan Institute of Chemical Physics NAS RA, 5/2 P. Sevak Str., Yerevan 0014, Armenia; mkrtich.yeranosyan@gmail.com

[3] Instituto de Alta Investigación, Universidad de Tarapacá, Casilla 7D, Arica 1000000, Chile; dlarozen@academicos.uta.cl

* Correspondence: manuk.barseghyan@nuaca.am

Abstract: This study investigated how the water–cement ratio and silica fume concentration affect the compressive strength of cement mortars. This comprehensive study delved into the intricate interplay between water–cement ratio and silica fume concentration, examining their influence on cement-based mortars' compressive strength and water absorption characteristics. The silica fume concentration was investigated, ranging from 5% to 15% of the cement weight. The investigation employed two distinct mixing techniques, mixing cement and silica fume, before extracting appropriate samples; alternatively, a magnetic stirrer was used to prepare samples by dissolving silica fume in water. The cement mortars were also prepared with three different water–cement ratios: 0.44, 0.47, and 0.5. The interesting findings of compressive tests illuminated a consistent trend across all curing days and mixing methods—a reduction in the water–cement ratio corresponded with a notable increase in compressive strength. However, it is essential to note that the influence of the mixing method on the compressive strength of cement-based mortars is based on the water–cement ratio. The results show that by using the suggested technological method, it was observed that samples prepared with water–cement ratios (W/C) of 0.47 and 0.44 exhibited higher compressive strengths compared to those prepared using the well-known standard mixing method. The compressive test results underscored that the water–cement ratio reduction consistently enhanced the compressive strength in every combination of curing days and mixing techniques. Furthermore, this reduction in the water–cement ratio was correlated with a decrease in water absorption of the mortar. Conversely, the water–cement ratio itself played a pivotal role in defining how the mixing technique affected the compressive strength and water absorption of cement-based mortars. This multifaceted exploration underscores the nuanced relationships between key variables, emphasizing the need for a comprehensive understanding of the intricate factors influencing the mechanical and absorptive properties of cement-based materials.

Keywords: silica fume; cement mortar; mixing method; compressive strength; water absorption

Citation: Badalyan, M.M.; Muradyan, N.G.; Shainova, R.S.; Arzumanyan, A.A.; Kalantaryan, M.A.; Sukiasyan, R.R.; Yeranosyan, M.; Laroze, D.; Vardanyan, Y.V.; Barseghyan, M.G. Effect of Silica Fume Concentration and Water–Cement Ratio on the Compressive Strength of Cement-Based Mortars. *Buildings* **2024**, *14*, 757. https://doi.org/10.3390/buildings14030757

Academic Editors: Abderrahim Boudenne and Hamza Allam

Received: 19 January 2024
Revised: 13 February 2024
Accepted: 1 March 2024
Published: 11 March 2024

1. Introduction

Concrete, a pivotal material in civil engineering, has found extensive application in both industrial and civil construction over the decades. Concrete is renowned for its commendable performance and prolonged durability. As a heterogeneous and brittle material, cement-based mixtures, particularly those exposed to difficult environmental conditions, are prone to physical, chemical, and biological erosion. Factors such as chloride

ions, water, carbon dioxide, and sulfate contribute to erosion, resulting in a decline in performance or a reduction in the overall service life [1]. Rather than being a waste product, silica fume has been accepted as a by-product of the silicon metal and ferro-silicon alloy industries and is of excellent quality for the cement and concrete industries. The term "silica fume" is used in the European standard [2], though it is also known by other names such as microsilica, volatilized silica, condensed silica fume, and silica dust.

Silica fume is a highly reactive pozzolanic material [3–5] due to its extreme fineness and high content of amorphous silicon dioxide. Its effects are related to the following factors: reduction in alkali–silica reactivity, creep rate, freeze–thaw durability, coefficient of thermal expansion, dielectric constant, specific heat, dynamics of defect formation, thermal conductivity, strength, ductility, modulus, vibration damping capacity, sound absorption, abrasion resistance, air void content, bonding strength with reinforcing steel, shrinkage, permeability, resistance to chemical attack, corrosion resistance of embedded steel reinforcement, and degree of fiber dispersion in mixes containing short microfibers [6–19].

In silica fume, trace amounts of iron, magnesium, and alkali oxides can also be identified. Silica fume is available in two color variations: premium white or grey. The literature on silica fume and silica fume concrete exceeds 3000 publications. Its utility as a material for supplementary cementitious purposes has been widely explored to enhance strength and durability [20–23]. The mechanism of silica fume in mortar and concrete can be delineated through three primary functions: refinement of pore size and matrix densification, reaction with free lime, and refinement of the cement paste–aggregate interfacial zone. According to Igarashi et al., ordinary concrete with silica fume had less coarse pores than regular concrete, even within the first 12 and 24 h [24].

When silica fume is incorporated into concrete mixtures, it significantly alters the compressive strength, primarily through the improvement in the aggregate–paste bond and the enhancement in the microstructure. This enhancement primarily results from the improved bond between the aggregates and paste, as well as the refinement of the microstructure. In a study by Mazloom et al., the effect of silica fume (at concentrations of 0%, 6%, 10%, and 15%) on the compressive strength of high-performance concrete was investigated over 400 days, with concentrations ranging from 0% to 15%. The findings revealed that at 28 days, the compressive strength of silica fume concrete exceeded that of the control concrete by 21%, highlighting the positive influence of silica fume. However, beyond the 90 days, the development of compressive strength in concrete mixtures containing silica fume showed negligible changes [25]. The ongoing investigation into the multifaceted contributions of silica fumes and their lasting effects on concrete properties remains a focal point in construction materials research.

In a recent comprehensive investigation, an upward trend in plastic shrinkage strain was observed with increasing dosages of silica fume. Furthermore, this study highlighted that silica fume played a mitigating role in reducing creep strain compared to concrete prepared solely with Portland cement, with this effect being discernible across varying dosage levels of silica fume [26–29]. The nuanced understanding gained from this research sheds light on the intricate relationship between silica fume dosage and the mechanical properties of concrete, particularly plastic shrinkage and creep.

Expanding on the implications of the findings, it was explained that silica fume exhibits a significant enhancement in water resistance and possesses robust pozzolanic activity. This characteristic renders it a valuable addition to concrete compositions, with the potential to enhance the creation of durable structures [30]. The incorporation of silica fume into concrete not only improves specific mechanical properties but also enhances the durability and stability of the resulting structures, as shown in the results of this study. It highlights the multi-faceted benefits that silica fume brings to the field of concrete technology and its role in the search for environmentally friendly and durable building materials.

Cement mortar is a composite substance with distinct characteristics determined by the proportions of its constituents [31]. Various parameters influence the mechanical prop-

erties of cement mortar, including the water–cement ratio [32], age [33], sand-to-cement ratio [34], and admixtures [35]. Numerous experimental studies have investigated the relationship between the water–cement ratio and the mechanical properties of cement mortar. Haach et al. [36] observed that a higher water–cement ratio reduces both compressive and flexural strength. Several studies have investigated the impact of ageing on concrete, with findings indicating an enhancement in mechanical properties with increasing age [37–39]. Li et al. [32] noted that the demand for superplasticizers increases with the increase in strength resulting from a reduction in the water–cement ratio or the addition of silica fume and nanosilica. It is noteworthy that silica fume can enhance the volume stability (soundness) of concrete mixtures [40,41].

This research extensively explores the effects of both the water–cement ratio and the concentration of silica fume on the compressive strength and water absorption characteristics of cement-based mortars. The primary focus of the investigation was on silica fume concentrations, particularly at 5%, 10%, and 15% relative to the cement weight. To ensure a comprehensive analysis, two distinct mortar preparation techniques were employed. In the first approach, cement and silica fume were meticulously blended together, and subsequently, samples were molded and then carefully extracted for evaluation. As an alternative method, a magnetic stirrer was used for a different mixing procedure, wherein silica fume was dissolved in water to form the mortar samples. This dual-pronged method was adopted to ensure a robust assessment of the influence of silica fume concentration on the properties of cement-based mortars. By delving into these diverse mixing techniques and silica fume concentrations, this study aimed to provide a nuanced understanding of their impact on compressive strength and water absorption, thus contributing valuable insights to the broader field of cement-based materials research.

2. Materials and Methods

2.1. Materials

The binder used in the investigation was ordinary Portland cement 52.5 (GOST 31108-2020) from the Armenian Ararat Cement Factory. Table 1 presents the chemical composition and physical parameters of the cement used in compliance with EN 196-2:2002 [42,43], EN 196-3:2002 [44], and GOST EN 196-1:2002 [45]. Table 2 comprehensively outline the physical and chemical properties of the sand, used in this study. The silica fume, sourced from the "EFFECT GROUP" in Yerevan, Armenia, serves as an additive in these mortars. It is an amorphous form of silicon dioxide (SiO_2) produced as a byproduct in the production of silicon metal and ferrosilicon alloys.

Table 1. Physical properties of cement.

Characteristics	Days	Results Obtained
Standard consistency (%)	-	28
Specific gravity (g/cm^3)	-	3.1
Blaine fineness (cm^2/g)	-	4552
Compressive strength (MPa)	3 days	21
	7 days	38
	28 days	52
Setting time (min)	Initial	55
	Final	325

Chemical composition of cement (wt.%)								
Al_2O_3	SiO_2	Fe_2O_3	CaO	MgO	SO_3	Loss on ignition	Insol. Residue	Free CaO
4.5	21.9	2.17	61.6	1.1	2.1	3.2	1.9	1.5

Table 2. Physical properties of sand.

Fineness Modulus	Specific Gravity	Zone	Bulk Density in Compact State (kg/m^3)	Bulk Density in Loose State (kg/m^3)
2.35	2.50	II	1641	1470

The Fourier transform infrared (FTIR) spectrum depicted in Figure 1 for silica fume serves as a valuable tool for elucidating insights into its molecular structure and vibrational modes. Within the intricate patterns of the FTIR spectra associated with silica fume, discernible bands emerge, each indicative of specific stretching and bending vibrations inherent in the Si-O bonds. The nuanced positioning of these bands proves to be a dynamic aspect, subject to variation contingent upon several factors. Paramount among these factors is the distinctive production process employed, which introduces a range of influences on the molecular arrangement and vibrational characteristics of the silica fume. Furthermore, the amorphous nature of the silica fume also exerts a discernible impact on the precise locations of these vibrational bands in the FTIR spectrum. The FTIR analysis of silica fume becomes a sophisticated avenue for not only discerning the molecular intricacies but also for unravelling the intricate dance of Si-O bond vibrations. The spectrum thus emerges as a nuanced canvas, capturing the nuanced interplay of factors shaping the molecular landscape of silica fume and contributing to the multifaceted characteristic of its vibrational features. As shown in Figure 1, the bands at 456 cm^{-1} and 802 cm^{-1} were assigned to the bending vibration of O–Si–O and symmetric stretching of Si–O–Si, respectively. The strong band at 958–1270 cm^{-1} belonged to the asymmetric stretching modes of Si–O bonds. The FTIR vibrational modes of silica fume were associated with the structural configurations of Si–O bonds. The absorption bands at 1063.3, 1129.0, and 1172.2 cm^{-1} were associated with the asymmetric stretching modes of the Si–O bonds.

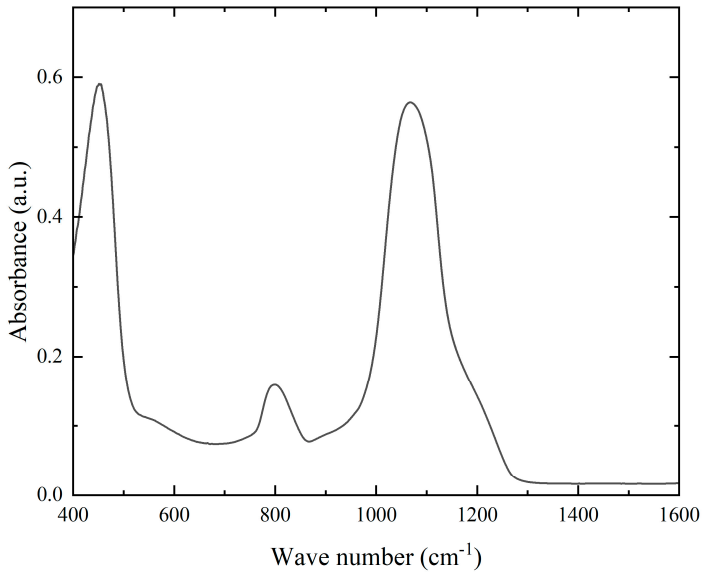

Figure 1. The FTIR spectra of the aforementioned silica fume.

Scanning electron microscopy (SEM) is a powerful imaging technique that uses electrons to create high-resolution images of a sample's surface. When examining silica fume using SEM, it is possible to gain valuable insights into the morphology and size distribution of the particles. Here is the most important point regarding SEM images of silica fume: silica fume particles typically exhibit a spherical morphology, resembling tiny spheres or agglomerates of spheres. The high magnification capabilities of SEM allow for detailed observation of the surface features and structure of individual particles (Figure 2).

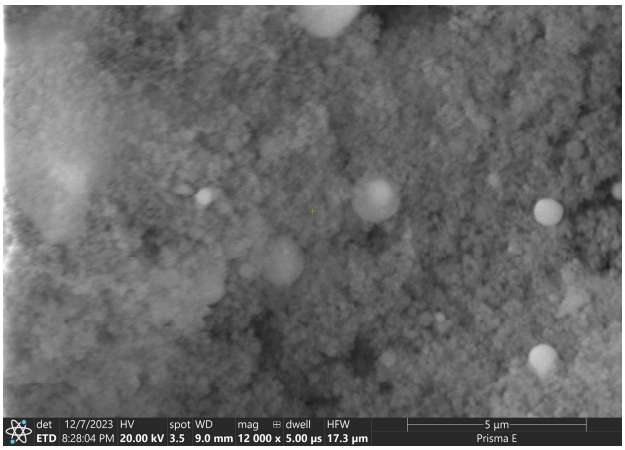

Figure 2. SEM image of silica fume.

2.2. Mixing and Sample Preparation

The primary objective of this study was to investigate the influence of silica fume and variations in the water–cement ratio on the compressive strength of a Portland cement composite material, incorporating an effective mineral additive. Additionally, we examined changes in the technological scheme for preparing the mixture, particularly focusing on the sequence of mixing the components.

In this study, to obtain a highly effective cement composite with increased corrosion resistance and durability, silica fume was selected from the various existing mineral modifiers (RA is rich in amorphous aluminosilicate rocks, which are widely used as hydraulic additives), of various doses—5, 10, and 15% by weight of Portland cement M500 (class 52.5 N)—and river sand from the Ranchpar deposit as a filler.

Two techniques for producing mortar mixtures were investigated: in the first case, silica fume was mixed with the sand, while in the second case, it was used as a suspension. Beam samples measuring 40 × 40 × 160 mm were prepared from the cement-based mortar, comprising Portland cement and river sand in a ratio of 1:2.5; or more precisely, to prepare 6 beam samples, 880 g of Portland cement M500 and 2200 g of sand were utilized.

In the first mixing method, Portland cement and silica fume were mixed for three minutes, followed by the addition of sand. The mixture was then stirred for an additional minute without adding water. Once a homogeneous dry mixture was achieved, the required amount of water was added, and stirring continued for an additional five minutes to produce a homogeneous mortar mixture. In the second mixing method, the mixing of water and silica was performed with a magnetic stirrer (rotation speed 800 rpm, maximum power of 145 W) for 5 min. Silica was gradually added to water on a magnetic stirrer over 1.5 min, followed by continued co-mixing for 3.5 min.

The resultant mixes were molded into beam samples using a vibrating table (C278, Matest, Treviolo, Italy) in less than a minute. In the second mixing method, the components were mixed in a different order. Portland cement and sand in a dry state were mixed for 2 min, and silica fume and water were stirred separately with a magnetic stirrer for 5 min until a suspension was obtained. The cement–sand mixture was mixed with the resulting suspension, and beam samples of the same size were formed from the resulting mixtures and compacted according to the same regime.

Figure 3 shows the entire process of preparing test samples. The characteristic steps of the starting materials included mixing water and silica with a magnetic stirrer and mixing the materials together in a mortar, resulting in cement mortar in prismatic metal molds of 40 mm × 40 mm × 160 mm dimensions. After 24 h, the test samples were removed from the mold and transferred to a chamber under normal conditions, where the temperature was (20 ± 2) °C and the humidity was (98 ± 2)%. After 28 days of storage under these conditions, the test specimens were removed from the water and subjected to testing. The compressive strength was determined for cube-shaped specimens with dimensions of

40 mm × 40 mm. The arithmetic mean of the test values of one batch, i.e., six test specimens, was taken as the compressive strength value according to EN196-1-2002, Point 10.2.

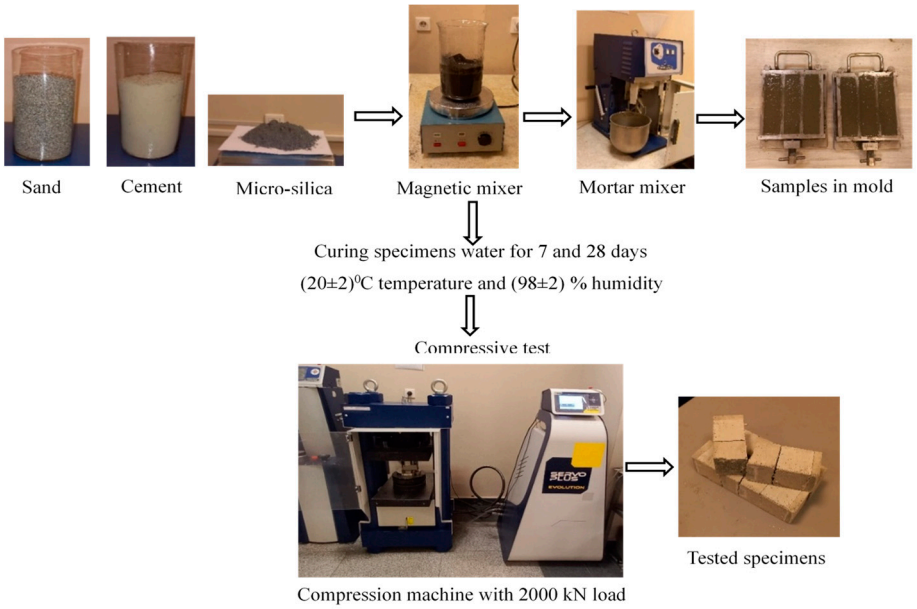

Figure 3. Diagram of the experimental procedure.

2.3. Compressive Strength Testing

For the comprehensive evaluation of compressive strength, a meticulous sampling approach was employed, with three samples randomly selected from each batch. The assessment of compressive strength was executed with precision using an advanced 2000 kN automatic concrete compression machine (Servo-Plus Progress, MATEST, Treviolo, Italy), adhering to the rigorous standards outlined in EN 196-1. Notably, the specimens subjected to compressive strength testing featured dimensions of 40 × 40 mm, ensuring a standardized and consistent evaluation process. The compressive tests were meticulously conducted at two crucial time points, specifically at the ages of 7 and 28 days. This critical examination was facilitated by the deployment of an automatic compression machine (C089, MATEST), characterized by a loading rate set at 2.4 kN/s. The deliberate choice of time intervals allowed for a nuanced understanding of the evolution of compressive strength over a defined period, contributing to a comprehensive understanding of the mechanical properties of concrete. Moreover, this multifaceted study encompassed an exploration of water absorption characteristics, adding a layer of depth to the overall analysis. The examination of water absorption followed stringent protocols as outlined in GOST 12730.3-2020 [46], ensuring a meticulous and standardized approach. This additional facet of the investigation provides valuable insights into the material's permeability and durability, enriching the overall understanding of the concrete's performance beyond its compressive strength. The methodical integration of diverse testing procedures and standards underscores the robustness of this study, yielding a comprehensive and nuanced portrayal of the concrete's mechanical and absorptive characteristics.

2.4. Water Absorption Calculation

Water absorption refers to the ability of material to absorb water when immersed in it and is represented with water absorbing capacity [46].

After being dried at 105 °C to a consistent weight, the test samples were weighed in an air-dried condition (m_1). The saturated test samples were immersed in a container of water maintained at a temperature of 20 ± 2 °C to determine their mass. The water level was maintained at 50 mm above the upper mark of the test samples. The test samples were weighed in the air at 24 h intervals with an accuracy of no more than 0.1% (m_2). The

samples are considered saturated when the variation in subsequent weights is less than or equal to 0.1%. Following the previously indicated procedures, the test samples' water absorption (W) was calculated using the formula:

$$W = \frac{m_2 - m_1}{m_1} \cdot 100\%,$$

where W is the mass water absorbing capacity (%); m_2 is the volume water absorbing capacity (%); and m_1 is the mass of material saturated with water (g).

3. Results and Discussion

The starting ratio of water to cement (W/C) in this study was 0.5. At 7 days, with the inclusion of silica fume in an amount of 5, 10, and 15% of cement mass, the compressive strength, compared with the strength of the reference sample, according to the first mixing method for preparing the mortar, increased by 24, 26.5, and 33.5%, respectively, and at 28 days, by 4, 16, and 21.1%, respectively. According to the second mixing method, the prepared mixture exhibited nearly twice the strength gain during the initial hardening period. At 7 days of age, the strength increased by 14.3, 19.8, and 30.6%, and in the second period, the dynamics were slightly worse. At 28 days, the strength increased compared with the reference sample by 12.6, 16.48, and 16.53%, respectively, but compared with the first method, the strength was lower. The dynamics of strength gain are presented graphically in Figure 4.

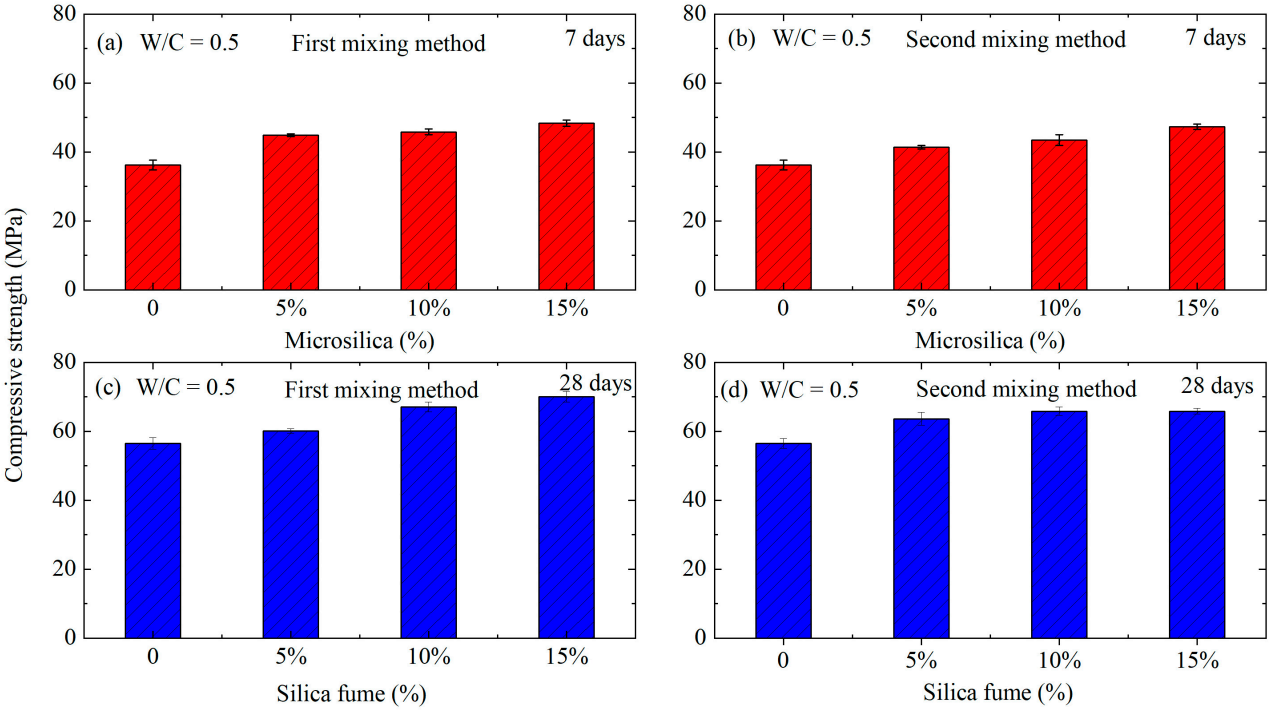

Figure 4. Compressive strength of the samples, where two different mixing methods are used and W/C = 0.5. The results are given for (**a**,**b**) 7 days and (**c**,**d**) 28 days.

The second batch of samples was prepared with W/C = 0.47 (reduction step 0.03), and the results are graphically presented in Figure 5.

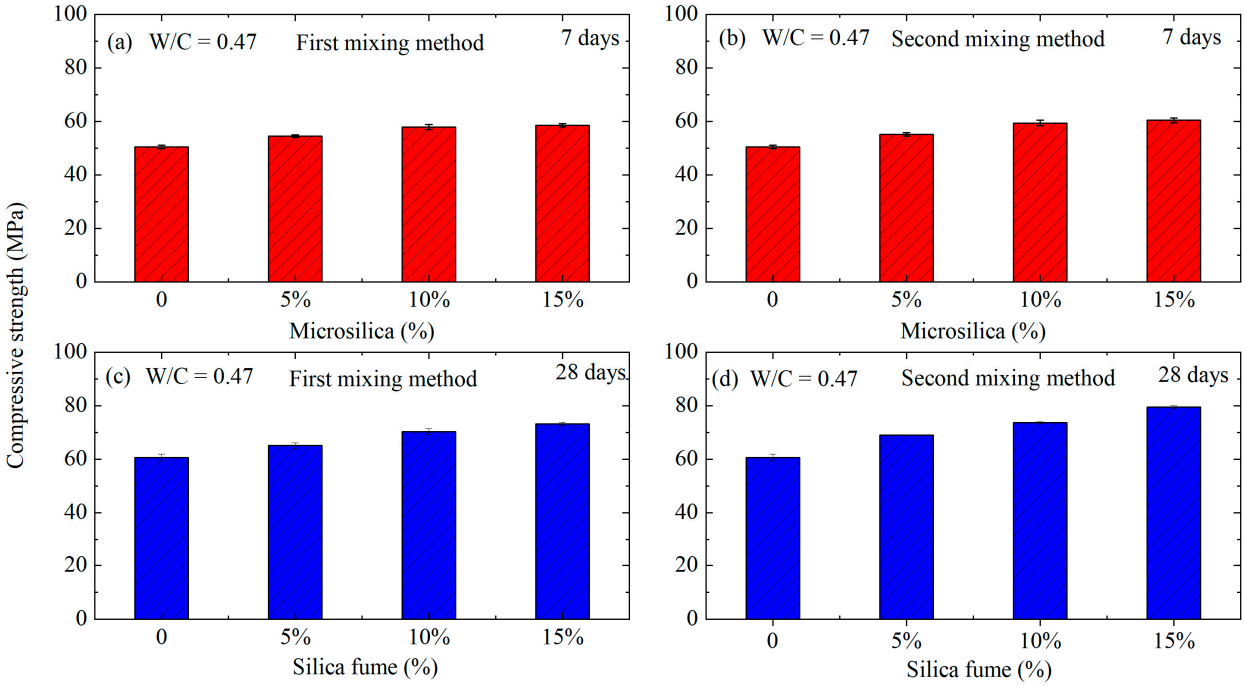

Figure 5. Compressive strength of samples in the case of two different mixing methods and W/C = 0.47. The results are given for (**a**,**b**) 7 days and (**c**,**d**) 28 days.

When we prepared cement-based mortar using the first technique (W/C = 0.44), with a silica fume content of 10 and 15%, the strength increased slightly (approximately 2%). According to the second mixing method, when silica fume was mixed with water for 5 min, the mortar became even harder, because, when mixed, microparticles form lumps (accumulations of particles), which capture part of the water, and the mixture becomes even harder and the compaction process becomes more difficult, which leads to a decrease in strength (Figure 6). At a water–cement ratio of 0.47, no drop in compressive strength is observed. With different methods of mixing the components, the results obtained were ambiguous, and the reason was a different water–cement ratio. At W/C = 0.5, the results obtained were better with the first mixing technology, when the components were mixed in a dry state and the silica fume was better distributed. Mixing silica in an excess amount of water contributed to the fact that some of the microsilica remained in lumps, i.e., dispersed worse. Reducing the amount of water led to the components of the mixture being in more confined conditions. Aggregated clumps dispersed better during the mixing process as they collided and rubbed against each other, leading to improved dispersion and the manifestation of pozzolanic activity. The optimal amount of microsilica amounted to 10% of the cement mass at W/C = 0.44. This contributes to the formation of a matrix with a denser structure, increasing the strength of the conglomerate. However, it is important to note that with an increased content of microsilica (15%), the concrete mixture became stiff, which hindered the compaction of the samples and led to a slight decrease in strength (by 0.7 MPa). To mitigate this undesirable effect, a comprehensive approach to modification is necessary, e.g., adding a plasticizer to silicon dioxide. The optimal amount of microsilica was 10% of the cement mass at W/C = 0.44. This contributes to the formation of a matrix with a denser structure, increasing the strength of the conglomerate. However, with an increased content of microsilica (15%), the concrete mixture became stiff, which hindered the compaction of the samples and led to a slight decrease in strength (by 0.7 MPa). To mitigate this undesirable effect, a comprehensive approach to modification is necessary, e.g., adding a plasticizer to silicon dioxide.

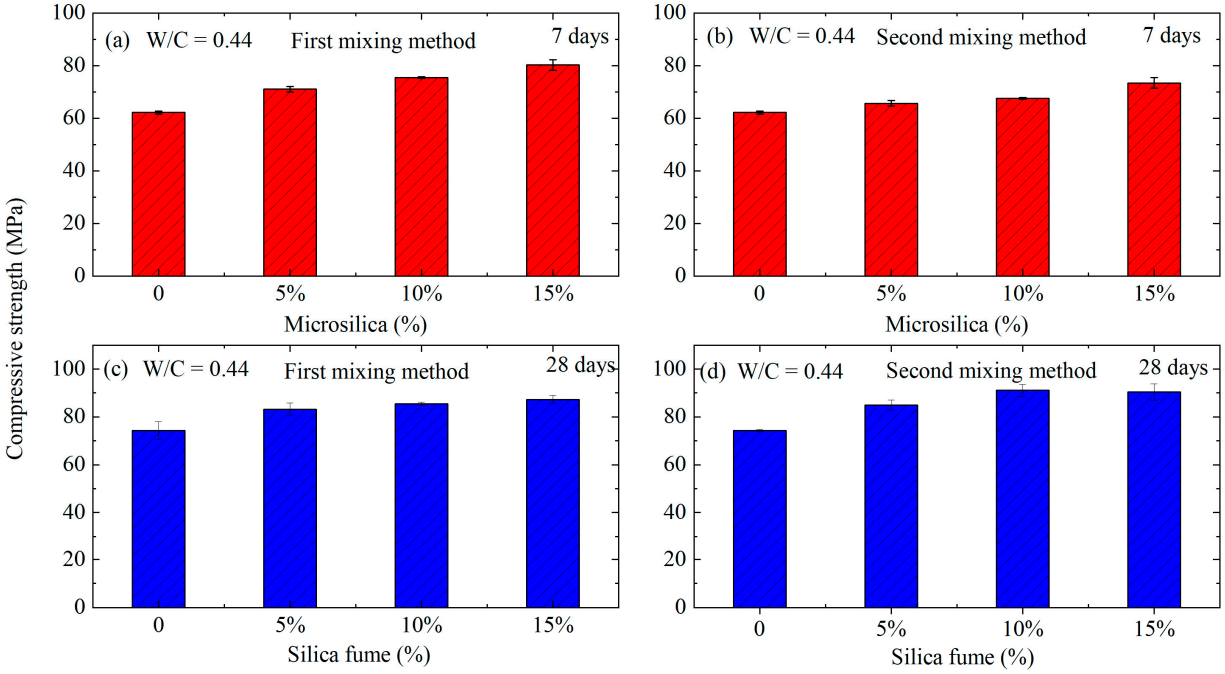

Figure 6. Compressive strength of samples in the case of two different mixing methods and W/C = 0.44. The results are given for (**a**,**b**) 7 days and (**c**,**d**) 28 days.

At the end of the induction period, when the paste loses its plasticity, the reactive amorphous silica fume, which lacks long-range order and is in a thermodynamically unstable state, undergoes a chemical interaction with calcium hydroxide (pozzolanic reaction), which forms during the hydrolysis of the main Portland cement mineral. Because of this chemical interaction, low–basic gel calcium silicate hydrate (CSH) is synthesized, which increases the density of the cement matrix and, consequently, the mortar. In the composition of the cement stone, there is a change in the balance between weakly hydrated phases and more stable and durable calcium silicate hydrates. By removing easily leachable calcium hydroxide from the cement matrix, the concrete becomes more resistant to aggressive operating conditions.

In the case of the first mixing method (a), with a water–cement ratio (W/C) of 0.5, the water absorption indicators of the samples decreased from 10% to 9.4% as the mass of silica increased (0%, 5%, 10%, and 15%). With W/C = 0.47, it decreased from 10.8% to 9.4%, and in the case of W/C = 0.44, it decreased from 9.6% to 6.1%. In the case of the second mixing method (b), with a water–cement ratio (W/C) of 0.5, the water absorption indicators of the samples decreased from 10% to 7.4% with the increase in the amount of silica (0%, 5%, 10%, and 15%). For 0.47 W/C, it decreased from 10.8% to 7.3%, and in the case of W/C = 0.44, it decreased from 9.5% to 6.6%.

According to these two mixing methods, a series of samples were prepared, wherein the water–cement ratio (W/C) was varied to 0.5, 0.47, and 0.44, along with different amounts of silica—5%, 10%, and 15% by the weight of Portland cement. All samples were cured under the same normal conditions in a wet state at a temperature of (20 ± 2) °C. Compressive strengths at 7 and 28 days, density, and water absorption were determined. It was found that a decrease in water absorption mainly increases the strength of the samples (Figure 7), which can be explained by a change in the nature of the porous structure. New formations that are synthesized during the reaction between silica fume and calcium hydroxide (formed during the hydrolysis of alite) slightly increase the average density of the solution (up to 10%), which leads to a reduction in pore volume and the strengthening of interpore walls. Density increases due to the compaction of the solution matrix, i.e., cement stone, which simultaneously increases the durability of the stone due to the removal of easily washed-out calcium hydrosilicate from the composition.

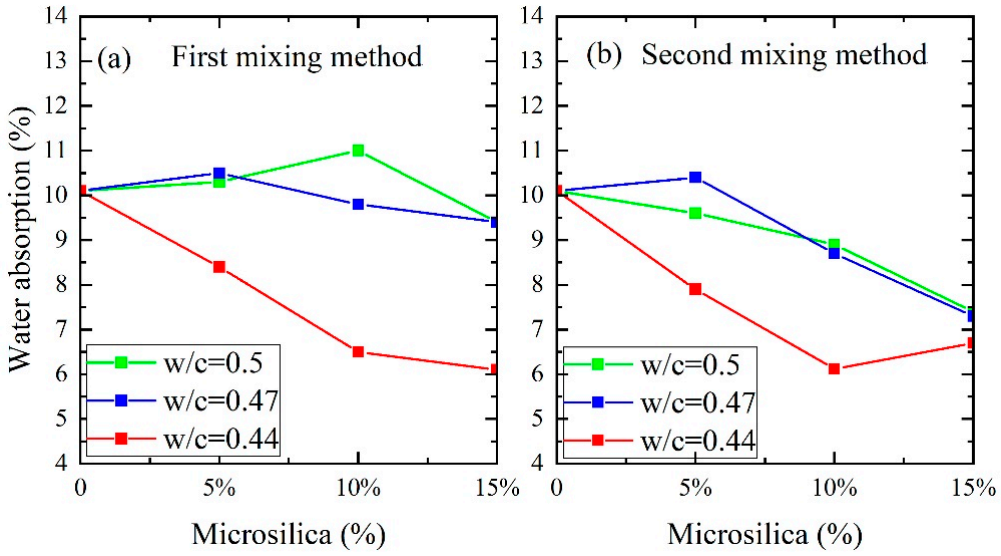

Figure 7. Water absorption of samples for two different mixing methods (**a**,**b**). Results are given for 28 days.

Compared to cement particles, silica fume has incredibly fine particles. These tiny particles enhance the packing density of concrete by filling the gaps between larger particles. The concrete's permeability is decreased by this denser packing, which also decreases the capillary pores' size and continuity. A byproduct of cement hydration, calcium hydroxide, reacts violently with silica fume. The cementitious matrix's density and connectivity are enhanced by the extra calcium silicate hydrate (CSH) gel that is created by this reaction. This densification further restricts the flow of water through the concrete. The linked pore structure is reduced because of the extra CSH gel production and cement matrix densification. This reduction in interconnected pathways limits the movement of water, thereby decreasing the permeability of concrete.

The addition of silica fume and the decrease in the water–cement ratio increase the physical and mechanical characteristics of the solution, especially at W/C = 0.44 with a silica fume content of 10%. Silica fume with a reduced water–cement ratio, located in cramped conditions, was better dispersed due to the collision and friction of lumps during the mixing process. With a good dispersion of silica fume, pozzolanic reactions between it and $Ca(OH)_2$ occur more intensively; low–basic hydrosilicates such as CSH are synthesized in greater quantities, which affect the porous structure of the matrix and, as a result, water absorption and permeability of the solution are reduced; and durability increases due to the removal of easily washed-out (especially in cold water) calcium hydroxide from the composition of the cement matrix.

4. Conclusions

This study investigated how the water–cement ratio and silica fume concentration affect the compressive strength of cement mortars. This comprehensive study delved into the intricate interplay between water–cement ratio and silica fume concentration, examining their influence on cement-based mortars' compressive strength and water absorption characteristics. The predicted and experimental findings are incorporated to reveal the following prominent conclusions:

1. In accordance with the second technological method, it was observed that samples prepared with water–cement ratios (W/C) of 0.47 and 0.44 exhibited higher compressive strengths compared to those prepared using the first method. However, this trend did not hold for the W/C ratio of 0.5. This phenomenon can be attributed to the inherent tendency of all mineral additives to aggregate, leading to a reduction in specific surface area. To address this, these additives are typically mixed either in

a dry state with other components or in water. Stirring silica fume with water, for instance, facilitates the separation of aggregated particles through wedging with water and collision impacts during the mixing process. However, it was noted that within 5 min, lumps of silica fume persisted in the suspension, diminishing its effectiveness.

2. Notably, at the lowest water–cement ratio (W/C = 0.44), the components of the mixture experience more constrained conditions. This contributes to the formation of a matrix with a denser structure, increasing the strength of the conglomerate. However, it is crucial to consider that at an increased silica fume content of 15%, the concrete mixture became rigid, making sample compaction challenging and leading to a slight decrease in strength (by 0.7 MPa). To mitigate this undesirable effect, a comprehensive modification approach is necessary, such as the addition of a plasticizer into silica.
3. Based on the aforementioned data, it can be concluded that the optimal composition is achieved with a W/C ratio of 0.44 and a silica fume content of 10% by the weight of cement, as per the second scheme. This formulation exhibited a 22.5% increase in strength compared to the base sample. Furthermore, it maintained a high pH environment, making this concrete suitable for reinforced concrete structures. This comprehensive analysis underscores the significance of the intricate interplay between water–cement ratio and silica fume content, highlighting the need for a nuanced approach to achieve optimal concrete properties.

Author Contributions: Conceptualization, M.M.B., M.G.B., Y.V.V. and A.A.A.; methodology, N.G.M. and R.R.S.; validation, M.G.B., N.G.M. and M.A.K.; formal analysis, M.G.B. and M.A.K.; investigation, N.G.M., M.A.K., A.A.A. and M.Y.; resources, Y.V.V.; data curation, N.G.M. and A.A.A.; writing—original draft preparation, M.G.B., R.S.S., A.A.A. and D.L.; writing—review and editing, R.S.S., M.A.K., M.G.B. and D.L.; visualization, M.G.B. and D.L.; supervision, M.G.B. and Y.V.V.; project administration, Y.V.V.; funding acquisition, Y.V.V. and M.G.B. All authors have read and agreed to the published version of the manuscript.

Funding: The authors would like to acknowledge the financial support of the Science Committee of the Republic of Armenia (Project no. 21AG-1C008).

Data Availability Statement: The data presented in this study are available upon request from the corresponding author.

Conflicts of Interest: The authors declare no conflicts of interest.

References

1. Scarfato, P.; Maio, L.D.; Fariello, M.L. Preparation and evaluation of polymer/clay nanocomposite surface treatments for concrete durability enhancement. *Cem. Concr. Compos.* **2012**, *34*, 297–305. [CrossRef]
2. Fuat, K.; Fatih, A.; Ilhami, Y.; Yus, S. Combined effect of silica fume and steel fiber on the mechanical properties of high strength concretes. *Constr. Build. Mater.* **2008**, *22*, 1874–1880. [CrossRef]
3. Khayat Kamal, H.; Mitchell, D. Transportation research board, self-consolidating concrete for precast, prestressed concrete bridge elements. *Technol. Eng.* **2009**, *91*. Available online: https://www.semanticscholar.org/paper/Self-Consolidating-Concrete-for-Precast,-Concrete-Khayat-Mitchell/2d75c789b391893c5574b183d66ffc6e2fc11007 (accessed on 15 January 2024).
4. ACI Committee 234. Guide for the use of silica fume in concrete (ACI 234R). *ACI Mater. J.* **1995**, *92*, 437–440.
5. Malhotra, V.M. Fly ash, slag, silica fume, and rice-husk ash in concrete: A review. *Concr. Int.* **1993**, *15*, 23–28.
6. Almusallam, A.A.; Beshr, H.; Maslehuddin, M.; Al-Amoudi, O.S.B. Effect of silica fume on the mechanical properties of low quality coarse aggregate concrete. *Cem. Concr. Compos.* **2004**, *26*, 891–900. [CrossRef]
7. Phan, L.T.; Carino, N.J. Effects of test conditions and mixture proportions on behavior of high-strength concrete exposed to high temperatures. *ACI Mater. J.* **2002**, *99*, 54–66. Available online: https://tsapps.nist.gov/publication/get_pdf.cfm?pub_id=860335 (accessed on 18 January 2024).
8. Sarshar, R.; Khoury, G.A. Material and environmental factors influencing the compressive strength of unsealed cement paste and concrete at high temperatures. *Mag. Concr. Res.* **1993**, *45*, 51–61. [CrossRef]
9. Poon, C.; Azhar, S.; Anson, M.; Wong, Y. Comparison of the strength and durability performance of normal and high-strength pozzolanic concretes at elevated temperatures. *Cem. Concr. Res.* **2001**, *31*, 1291–1300. [CrossRef]
10. Behnood, A.; Ziari, H. Effects of silica fume addition and water to cement ratio on the properties of high-strength concrete after exposure to high temperatures. *Cem. Concr. Compos.* **2008**, *30*, 106–112. [CrossRef]

11. Felicetti, R.; Gambarova, P.G. Effects of high temperature on the residual compressive strength of high-strength siliceous concretes. *ACI Mater. J.* **1998**, *95*, 395–406.
12. Chan, S.Y.N.; Peng, G.F.; Anson, M. Fire behavior of high-performance concrete made with silica fume at various moisture contents. *ACI Mater. J.* **1999**, *96*, 405–411.
13. Parrott, L.J. Production and properties of high-strength concrete. *Concrete* **1969**, *3*, 443–448.
14. Hoff, G.; Bilodeau, A.; Malhotra, V.M. Elevated temperature effects on HSC residual strength. *Concr. Int.* **2000**, *22*, 41–47.
15. Janotka, I.; Bagel, L. Pore structures, perm abilities, and compressive strength of concrete at temperatures up to 800 °C. *ACI Mater. J.* **2002**, *99*, 196–200.
16. Bentur, A.; Goldman, A. Curing effects, strength and physical properties of high strength silica fume concretes. *J. Mater. Civ. Eng.* **1989**, *1*, 46–58. [CrossRef]
17. Hooton, R.D. Influence of silica fume replacement of cement on physical properties and resistance to sulfate attack freezing and thawing, and alkali–silica reactivity. *ACI Mater. J.* **1993**, *90*, 143–152.
18. Castillo, C.; Durrani, A.J. Effect of transient high temperature on high strength concrete. *ACI Mater. J.* **1990**, *87*, 47–53.
19. Sanjayan, G.; Stocks, L.J. Spalling of high-strength silica fume concrete in fire. *ACI Mater. J.* **1993**, *90*, 170–173.
20. Khayat, K.H.; Aitcin, P.C. Silica Fume: A Unique Supplementary Cementations Material. In *Mineral Admixtures in Cement and Concrete*; Ghosh, S.N., Ed.; ABI Books Private Limited: Delhi, India, 1993; Volume 4, pp. 227–265.
21. Silica Fume Association. *Silica Fume Manual*; Silica Fume Association: Lovettsville, VA, USA, 2005.
22. Hsu, L.S.; Hsu, C.T. Complete stress–strain behavior of high-strength concrete under compression. *Mag. Concr. Res.* **1994**, *46*, 301–312. [CrossRef]
23. Bhanja, S.; Sengupta, B. Influence of silica fume on the tensile strength of concrete. *Cem. Concr. Res.* **2005**, *35*, 743–747. [CrossRef]
24. Igarashi, S.I.; Watanabe, A.; Kawamura, M. Evaluation of capillary pore size characteristics in high-strength concrete at early ages. *Cem. Concr. Res.* **2005**, *35*, 513–519. [CrossRef]
25. Mazloom, M.; Ramezanianpour, A.A.; Brooks, J.J. Effect of silica fume on mechanical properties of high-strength concrete. *Cem. Concr. Compos.* **2004**, *26*, 347–357. [CrossRef]
26. Brooks, J.J.; Cabrera, J.G.; Megat, J.M.A. Factors Affecting the Autogenous Shrinkage of Silica Fume High-Strength Concrete. In *Proceedings of the International Workshop on Autogenous Shrinkage of Concrete*; Japan Concrete Institute: Hiroshima, Japan, 1998; pp. 185–192.
27. Tao, Z.; Weizu, Q. Tensile creep due to restraining stresses in high-strength concrete at early ages. *Cem. Concr. Res.* **2006**, *36*, 584–591. [CrossRef]
28. Tazawa, E.; Yonekura, A.; Tanaka, S. Rate of Hydration and Drying Shrinkage of Condensed Silica Fume Mortar Prepared by Double Mixing. In Proceedings of the 3rd CANMET/ACI International Conference on Fly Ash, Silica Fume, Slag and Natural Pozzolans in Concrete, Trondheim, Norway, 19–26 June 1989; Alsali, M., Ed.; American Concrete Institute: Detroit, MI, USA, 1989; pp. 350–364.
29. Tazawa, E.; Miyazawa, S. Autogenous Shrinkage of Concrete and Its Importance in Concrete Technology. In Proceedings of the 5th International RILEM Symposium on Creep and Shrinkage of Concrete, Barcelona, Spain, 6–9 September 1993; E & FN Spon: London, UK, 1993; pp. 159–168.
30. Uddin, M.A.; Bashir, M.T.; Khan, A.M.; Alsharari, F.; Farid, F.; Alrowais, R. Effect of Silica Fume on Compressive Strength and Water Absorption of the Portland Cement–Silica Fume Blended Mortar. *Arab. J. Sci. Eng.* **2023**, 1–9. [CrossRef]
31. Su, Y.; Li, J.; Wu, C.; Wu, P.; Li, Z.-X. Influences of nano-particles on dynamic strength of ultra-high performance concrete. *Compos. B Eng.* **2016**, *91*, 595–609. [CrossRef]
32. Li, L.; Huang, Z.; Zhu, J.; Kwan, A.; Chen, H. Synergistic effects of micro-silica and nano-silica on strength and microstructure of mortar. *Constr. Build. Mater.* **2017**, *140*, 229–238. [CrossRef]
33. Kargari, A.; Eskandari-Naddaf, H.; Kazemi, R. Effect of cement strength class on the generalization of Abrams' law. *Struct. Concr.* **2019**, *20*, 493–505. [CrossRef]
34. Elaqra, H.; Godin, N.; Peix, G.; R'Mili, M.; Fantozzi, G. Damage evolution analysis in mortar, during compressive loading using acoustic emission and X-ray tomography: Effects of the sand/cement ratio. *Cem. Concr. Res.* **2007**, *37*, 703–713. [CrossRef]
35. Palacios, M.; Puertas, F. Effect of superplasticizer and shrinkage-reducing admixtures on alkali-activated slag pastes and mortars. *Cem. Concr. Res.* **2005**, *35*, 1358–1367. [CrossRef]
36. Haach, V.G.; Vasconcelos, G.; Lourenço, P.B. Influence of aggregates grading and water/cement ratio in workability and hardened properties of mortars. *Constr. Build. Mater.* **2011**, *25*, 2980–2987. [CrossRef]
37. De Vargas, A.S.; Dal Molin, D.C.; Vilela, A.C.; Da Silva, F.J.; Pavao, B.; Veit, H. The effects of Na_2O/SiO_2 molar ratio, curing temperature and age on compressive strength, morphology and microstructure of alkali-activated fly ash-based geopolymers. *Cem. Concr. Compos.* **2011**, *3*, 653–660. [CrossRef]
38. Yang, X.; Feng, Y.; Rong, H.; Liang, J.; Zhang, G.; Huang, Y. The leaching-deterioration properties and leaching mechanism of cement mortar under dry-wet cycles. *Constr. Build. Mater.* **2023**, *400*, 132672. [CrossRef]
39. Figueira, R.B.; Sousa, R.; Coelho, L.; Azenha, M.; de Almeida, J.M.; Jorge, P.A.S.; Silva, C.J.R. Alkali-silica reaction in concrete: Mechanisms, mitigation and test methods. *Constr. Build. Mater.* **2019**, *222*, 903–931. [CrossRef]
40. Mehta, P. History and Status of Performance Tests for Evaluation of Soundness of Cements. In *Cement Standards-Evolution and Trends*; ASTM STP663-EB; American Society for Testing and Materials: Philadelphia, PA, USA, 1977; pp. 35–60.

41. Kabir, H.; Hooton, R.D.; Popoff, N.J. Evaluation of cement soundness using the ASTM C151 autoclave expansion test. *Cem. Concr. Res.* **2020**, *136*, 106159. [CrossRef]
42. Arzumanyan, A.A.; Tadevosyan, V.G.; Muradya, N.G.; Navasardyan, H.V. Study of "Saralsk" Deposit for Practical Applications in Construction. *J. Arch. Eng. Res.* **2021**, *1*, 3–6. [CrossRef]
43. *GOST EN 196-1-2002*; Methods of Testing Cement. Part 1. Determination of Strength. Available online: https://www.armstandard.am/en/standart/5556 (accessed on 31 July 2023).
44. *GOST EN 196-2-2002*; Methods of Testing Cement. Part 2. Chemical Analysis of Cement. Available online: https://www.armstandard.am/en/standart/5557 (accessed on 31 July 2023).
45. *GOST EN 196-3-2002*; Methods of Testing Cement. Part 3. Determination of Setting Time and Soundness. Available online: https://www.armstandard.am/en/standart/5558 (accessed on 31 July 2023).
46. *GOST 12730.3-2020*; Concretes. Method of Determination of Water Absorption. Available online: https://www.armstandard.am/en/standart/5508 (accessed on 31 July 2023).